

HgI₂ As X-Ray Imager: Modulation Transfer Function Approach

Md.Ashikuzzaman¹, Jisan Ali¹, R. Adib², M.M. Hossain³, and Shaikh Asif Mahmood⁴

¹*Department of Electrical and Electronics Engineering, Daffodil International University, Dhaka-1207, Bangladesh*

²*Department of Technology, Harriken.com Limited, Dhaka-1213, Bangladesh*

³*Department of Firmware, Relisource Technologies Limited, Dhaka-1212, Bangladesh*

⁴*Department of Electrical and Electronic Engineering, Bangladesh University of Engineering and Technology, Dhaka-1000, Bangladesh*

ABSTRACT : *The Modulation Transfer Function (MTF) of Polycrystalline Mercuric Iodide based flat panel x-ray detectors is simulated as a function of spatial frequency. A simplified mathematical model for MTF is applied on four different published prototypes of Polycrystalline Mercuric Iodide. Our aim was to fit curve from MTF model with the curve from experimental data. The result of simulation from theoretical model shows a good agreement with the measured data. We have found that deep-trapping, K-fluorescence, dependence of dark current on temperature and exposure time are the most possible reasons for the slight mismatches between two curves. In addition, the mobility-lifetime product for best curve fitting was also examined for each prototype.*

KEYWORDS - *Dark current, Deep trapping, K-fluorescence, Modulation Transfer Function, Polycrystalline, Spatial frequency.*

I. INTRODUCTION

Flat panel digital x-ray image detectors are a class of solid-state x-ray digital radiography devices similar in principle to image sensors used in clinical photography [1,2]. Two types of commonly used flat panel detectors are in practice-direct conversion and indirect conversion. The direct conversion flat panel detector consists of a photoconductor layer sandwiched between two electrodes; the electrode at one surface is a continuous metal plate and the electrode at the other surface of the photoconductor is segmented into an array of individual square pixels held at ground potential. A bias voltage applied to the radiation-receiving top electrode results in an electric field in the photoconductor. Image irradiation causes a latent image charge accumulation on the pixel electrodes. Some of the x-ray generated charge carriers get trapped in the bulk of the photoconductor layer during their drift toward the electrodes. This trapped carrier induces charges not only on this pixel electrode but also on its neighboring consequently causing a lateral spread of information and hence a loss of image resolution [3].

Whatever photoconductor layer is used, the aim is to obtain an image of good resolution. Resolution refers to the ability of a radiographic imaging system record fine detail. Obviously, detail is an obvious pre-requisite for clinical images of excellent quality. Mathematically, The quality of image is determined by "Modulation Transfer Function" (MTF). MTF measures the efficiency of an imaging system such as a detector to resolve

(transfer) different spatial frequencies of information in an image. In other words, MTF is the relative signal response of the system as a function spatial frequency. In the measurement process of MTF, mobility-lifetime product of electrons and holes is a very important parameter as sensitivity of photoconductor greatly depends on the value of it.

Amorphous Selenium (a-Se), Poly crystalline-Mercuric Iodide (Poly-HgI₂), Lead Iodide (PbI₂) are the most commonly used photoconductor layer in photo-detection. In this study, a simplified mathematical model [4] for MTF is used on various Published [5] prototypes of Mercuric Iodide. The simulation results are compared to experimental data and a good agreement is found. At last, mobility-lifetime product for best curve fitting is determined for each prototype.

II. MODEL AND SIMULATION

Resolution or modulation transfer function is determined from Line Spread-Function. The Line Spread-Function (LSF) is defined as the sum of the spatial distribution of illuminance in the front and the back emulsion caused by a beam of x rays which passes through photoconductor slit [6]. Fourier transformation of the LSF gives the corresponding modulation transfer function (MTF). For mathematical model, we have used the Line Spread Function (LSF) which is explained by Kabir and others *et al* [4]. After fourier transform of the Line Spread Function, it is found that [4],

$$G(f) = \frac{F(\mu_b\tau_b' + \mu_i\tau_i')(\omega \operatorname{cosech}(\omega) - e^{-\alpha L}\omega \operatorname{coth}(\omega) - \alpha L e^{-\alpha L})}{\frac{\eta}{\alpha^2 L}(1 - \mu_b\tau_b'F\alpha)(1 + \mu_i\tau_i'F\alpha)(\alpha^2 L^2 - \omega^2)} + \frac{\mu_b\tau_b'F \left(e^{-\alpha L} - e^{-\frac{L}{\mu_b\tau_b'F}} \right)}{\frac{\eta}{\alpha}(1 - \mu_b\tau_b'F\alpha)} \quad (2)$$

$$\frac{(\mu_b\tau_b'F)^2 \left(\omega \operatorname{cosech}(\omega) - e^{-\frac{L}{\mu_b\tau_b'F}}\omega \operatorname{coth}(\omega) - \frac{L}{\mu_b\tau_b'F}e^{-\frac{L}{\mu_b\tau_b'F}} \right)}{\frac{\eta}{\alpha L}(1 - \mu_b\tau_b'F\alpha)(L^2 - \omega^2\mu_b^2\tau_b'^2F^2)}$$

$$+ \frac{\left(e^{-L\left(\alpha + \frac{1}{\mu_i\tau_i'F}\right)}\omega \operatorname{cosech}(\omega) - e^{-\alpha L}\omega \operatorname{coth}(\omega) + \frac{L}{\mu_i\tau_i'F}e^{-\alpha L} \right)}{\frac{\eta}{\alpha L}(1 + \mu_i\tau_i'F\alpha)\left(\left(\frac{L}{\mu_i\tau_i'F}\right)^2 - \omega^2\right)}$$

$$+ \frac{\mu_b\tau_b'F \left(e^{-\alpha L} - e^{-\frac{L}{\mu_b\tau_b'F}} \right)}{\frac{\eta}{\alpha}(1 - \mu_b\tau_b'F\alpha)} \quad (1)$$

Where, μ_b is mobility of hole, μ_i is mobility of electron, τ_b' is lifetime of hole, τ_i' is lifetime of electron, α is linear attenuation co-efficient, F is the applied field, L is detector thickness. $\eta = 1 - e^{-\alpha L}$ is the quantum efficiency of the detector. ω is the angular frequency and $\omega = 2\pi f$ where f is spatial frequency.

At zero spatial frequency, the expression for $G(f=0)$ is [4]:

$$G(0) = \frac{F(\mu_b\tau_b' + \mu_i\tau_i')(1 - e^{-\alpha L} - \alpha L e^{-\alpha L})}{\eta L(1 - \mu_b\tau_b'F\alpha)(1 + \mu_i\tau_i'F\alpha)}$$

$$\frac{\left(\frac{\mu_b\tau_b'F}{L}\right)^2 \left(1 - \frac{L}{\mu_b\tau_b'F}e^{-\frac{L}{\mu_b\tau_b'F}} - e^{-\frac{L}{\mu_b\tau_b'F}}\right)}{\frac{\eta}{\alpha L}(1 - \mu_b\tau_b'F\alpha)}$$

$$+ \frac{\left(\frac{\mu_i\tau_i'F}{L}\right)^2 \left(e^{-L\left(\alpha + \frac{1}{\mu_i\tau_i'F}\right)} + \frac{L}{\mu_i\tau_i'F}e^{-\alpha L} - e^{-\alpha L} \right)}{\frac{\eta}{\alpha L}(1 + \mu_i\tau_i'F\alpha)}$$

Then, MTF due to bulk trapping [4] is,

$$MTF_{trap}(f) = \frac{G(f)}{G(0)} \quad (3)$$

The dataset which we have used was formed from an experiment where fabrication of polycrystalline HgI₂ film was performed by real-time radiography using two low temperature deposition methods—Physical Vapour Deposition (PVD) and Particle-in-Binder (PIB) deposition [5]. The experimenters performed PVD deposition in a vacuum reactor where high purity HgI₂ powder was evaporated and deposited on arrays. PIB deposition involves grains of purified HgI₂ crystals (~6.36 g cm⁻³) mixed with a polymer binder material (~1.05 g cm⁻³), with a composition ratio of 9 to 1 by weight for the two materials [5]. In this study, we have worked on four publicly available prototypes of Poly-HgI₂ namely PVD #4, PVD #12, PVD #16 and PIB #2 [5].

III. RESULT AND DISCUSSION

We start with the simulation of PVD #4 where detector thickness is 210 μm and electric field strength is .24 μm^{-1} . In case of PVD #4 (Fig.1), MTF values from theoretical model are very close to experimental data at high frequency region. For the simulation of PVD #12, detector thickness is 280 μm and electric field strength is .25 μm^{-1} . It is observed from the fitting curve of PVD #12 (Fig.2) that MTF values from theoretical model shows very good agreement with experimental data at low frequency region.

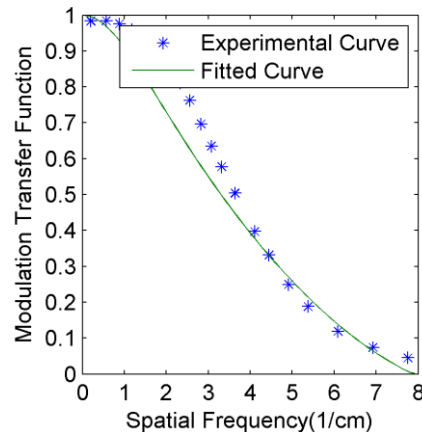


Fig.1. Fitting a curve for PVD #4 with thickness 210 μm and electric field strength .24 $\text{V } \mu\text{m}^{-1}$

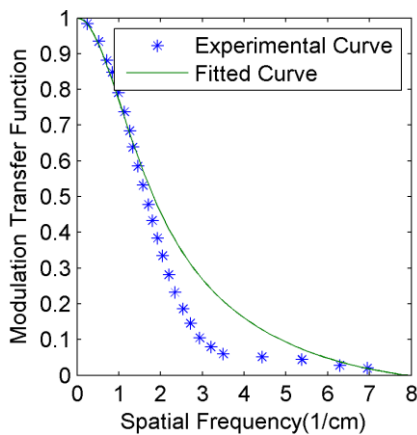


Fig.2. Fitting a curve for PVD #12 with thickness 280 μm and electric field strength $.25 \text{ V } \mu\text{m}^{-1}$

For the simulation of PVD #16, the detector thickness is 280 μm and the electric field strength is $.54 \mu\text{m}^{-1}$. In case of PVD #16(Fig.3), MTF values from theoretical model are very close to experimental data at neither low nor high frequency region rather in the medium values of frequency. The simulation of PIB #2 was performed at detector thickness 615 μm and electric field $.36 \mu\text{m}^{-1}$. When we come to study the case of PIB #2(Fig.4),we observe that fitting characteristics here are almost similar to PVD #16.

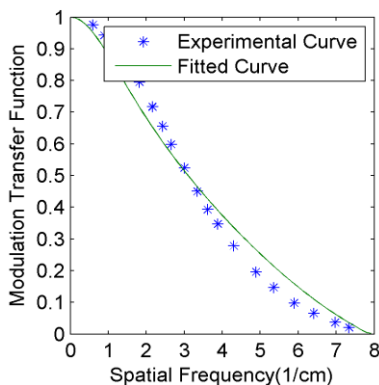


Fig.3. Fitting a curve for PVD #16 with thickness 280 μm and electric field strength $.54 \text{ V } \mu\text{m}^{-1}$

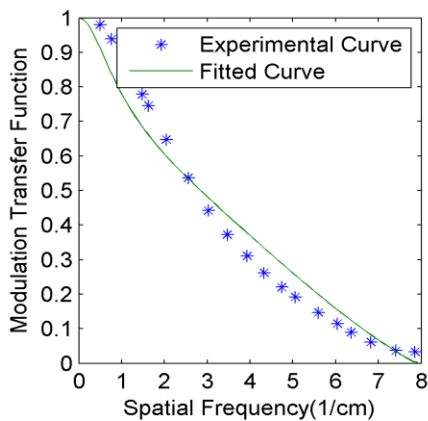


Fig.4. Fitting a curve for PIB #2 with thickness 615 μm and electric field strength $.36 \text{ V } \mu\text{m}^{-1}$

Irregular electron-hole pair generation at the depletion region causes dark current, resembling a noise in photoelectric devices. We have used a simplified model of MTF and dark current was not taken into consideration[4]. However, the existence of dark current would affect the experimental data resulting in slight mismatch between experimental curve and our model. In the MTF model, the exposure time is not considered though dark current generation has practical dependence on exposure time[7]. Several studies have shown that dark current also depends on temperature[7] which was not taken into account in the model we employed. These simplifications contribute to mismatch between experimental and theoretical data.

Some of the x-ray generated carriers are captured by deep traps in the bulk of the photoconductor during their drift across the photoconductor. The random nature of carrier charge trapping creates additional noise. This additional noise creates signal blurring. The trapped carriers reduce signals for the corresponding pixel and induce charge in the neighbouring pixels. Consequently, there is a lateral spread of induced charges in the pixels which affects image resolution[8]. This is an important reason for mismatch between theoretical and practical data as deep trapping is not considered in the mathematical model we used. Along with the stated factors, another reason which may contribute to the mismatch is the K-fluorescence phenomena. K-fluorescence is the emission of secondary x-ray resulting from bombarding high-energy x-ray. The K-fluorescent x-ray photon can be absorbed at a point different from the x-ray absorption site which deteriorates the image quality. We have used a model which does not take into account the K-fluorescence phenomena whereas in practical cases, K-fluorescence phenomena has significant effect on MTF performance[8].

The X-ray sensitivity of pixelated X-ray detectors greatly depends on the mobility and lifetime product of charges that move towards the pixel electrodes and the extent of dependence increases with decreasing pixel per unit detector thickness[9]. Table I shows the mobility-lifetime product for best fitting of the curves.

Table 1: Summary of the mobility- lifetime product For Best result of curve fitting in this study.

Prototype	Electric field strength (V μm^{-1})	Thickness (μm)	Mobility-lifetime product(cm^2/V)
PVD #4	.24	210	Electron: 0.9×10^{-6} Hole: 0.9×10^{-8}
PVD #12	.25	280	Electron: 10^{-4} Hole: 5×10^{-8}
PVD #16	.54	280	Electron: 10^{-5} Hole: 5×10^{-7}
PIB #2	.36	615	Electron: 10^{-6} Hole: 0.3×10^{-5}

IV. CONCLUSION

In summary, the MTF model applied to polycrystalline HgI₂ based x-ray image detectors shows a very good agreement with experimental data available. Fitting Characteristics of four prototypes are compared. The slight mismatches of theoretical and experimental data can be attributed to the dependence of dark current on exposure time and temperature, carrier random charge trapping, K-fluorescence phenomena. The mobility-lifetime products for best fitting for four prototypes have also been obtained. To investigate further with more accuracy and precision, an MTF model taking temperature dependence, multiple exposure, deep trapping and fluorescence phenomena into consideration could be studied.

REFERENCES

- [1] D.C. Hunt, O. Tousignant, Y. Demers, L. Laperriere, and J.A. Rowlands, "Imaging performance of amorphous selenium flat panel detector for digital fluoroscopy", *Proc. SPIE*, 5030, 2003, 226-234.
- [2] M. Zahangir Kabir, S.O. Kasap, and J.A. Rowlands, "Photoconductors for X-ray image sensors", in the Springer handbook of electronic and optoelectronic materials, Eds: S.O. Kasap and P. Capper, Springer 2005.
- [3] M.Z. Kabir, L. Chowdhury, G. Decrescenzo, O. Tousignant, S.O. Kasap, and J.A. Rowlands, "Effect of repeated x-ray exposure on the resolution of amorphous selenium based x-ray imagers", *Medical Physics*, 37(3), 2010, 1339-1349.
- [4] M. Zahangir Kabir and S.O. Kasap, "Modulation transfer function of photoconductive x-ray image detectors: effects of charge carrier trapping", *J. Phys. D: Apply. Phys.*, 36, 2003, 2352-2358.
- [5] Hong Du, Larry E Antonuk, Youcef El-Mohri, Qihua Zhao, Zhong Su, Jin Yamamoto, and Yi Wang, "Investigation of the signal behavior at diagnostic energies of prototype, direct detection, active matrix, flat-panel imagers incorporating polycrystalline HgI₂", *Phys. Med. Biol.* 53, 2008, 1325-1351.

[6] G. Lubberts, "The line spread function and the modulation transfer function of x-ray fluorescent screen-film systems-problems with double-coated films", *American Journal of Roentgenology*, 105, 1969, 909-917.

[7] G. Zentai, L. Partain, R. Pavlyuchkova, C. Proano, B. N. Breen, A. Taieb, O. Dagan, M. Schieber, H. Gilboa, and J. Thomas, "Mercuric iodide medical imagers for low exposure radiography and fluoroscopy", *Proc. SPIE*, 5368, 2004, 200-210.

[8] M.Z. Kabir, M.W. Rahman, and W.Y. Shen, "Modelling of detective quantum efficiency of direct conversion x-ray detectors incorporating charge carrier trapping and K-fluorescence", *IET Circuits Devices Syst.*, 5(3), 2011, 222-231.

[9] R. C. Whited and L. van den Berg, "Native defect compensation in HgI₂ crystals", *IEEE trans. Nuc. Sci.*, 24(1), 1977, 165-167.